XLIII
CILAMCE
21–25, November, 2022
FOZ DO IGUAÇU - PR - BRAZIL

Numerical analysis of the cold start of a distribution transformer filled with biodegradable oil

Garelli, L.[1], Ríos Rodriguez, G.A.[1], Storti, M. A.[1], Amadei, M.[2] , Ortiz, A [3].

[1]*Centro de Investigación de Métodos Computacionales (CIMEC) - UNL/CONICET. Predio CONICET Santa Fe, Colectora Ruta Nac. 168, Km 472, Paraje El Pozo, 3000, Santa Fe, Argentina.*
lucianogarelli@gmail.com
[2]*Tadeo Czerweny S.A. Bv. Argentino 160 (S2252CMP) Gálvez, Santa Fe, Argentina.*
[3]*Electrical and Energy Engineering Department, E.T.S. de Ingenieros Industriales y de Telecomunicación, University of Cantabria. Avenida de Los Castros, 39005 Santander, Cantabria, Spain.*

Abstract. This work presents a numerical analysis of the cold start of a distribution transformer filled with biodegradable oil in order to obtain a detailed description of temperatures and velocities distributions inside the transformer. When the transformer is placed in very extreme conditions, like in a wind farm with very low ambient temperature, and is filled with biodegradable oil the pour point of the oil can be reached. This type of analysis has not been necessary since mineral oils have very low pour point temperatures, below $-40\,°C$, but in the case of conventional sunflower oil can be $-18\,°C$. When the transformer is started from a temperature near the pour point the fluidity and hence the natural convection phenomena, which is the principal mechanism of the heat transportation inside the transformer, can be dramatically reduced. This reduction can lead to a local increase in the oil temperature, principally in the windings oil channels. In this work, several working temperatures are analyzed for a transformer with a rated power of 315 kVA and a voltage ratio of 13.2kV/0.4kV filled with biodegradable oil, through three-dimensional thermo-fluid dynamics simulations using the multiphysics scientific code Code_Saturne. This work is carried out as part of the EU Horizon 2020 BIOTRAFO project.

Keywords: Biodegradable oil, Distribution transformer, Computational Fluid Dynamics, Conjugate heat transfer.

1 Introduction

In this work, a thermo-fluid dynamic analysis during a cold start of an Oil-Natural Air-Natural (ONAN) distribution transformer filled with biodegradable oil is carried out. The main objective of this study is to compare the thermal and fluid dynamic behavior inside the transformer when the operating temperature is close to the oil pour point. The distribution transformer under analysis has a rated power of 315 kVA with a voltage ratio of 13.2kV/0.4kV. Distribution transformers are usually located within the urban areas, close to the citizens, so it is desirable to use natural or synthetic esters to cool the active parts instead of mineral oils, to minimize the environmental impact. Esters oils have several advantages, like better dielectric strength, higher water saturation point, and higher fire point among others when it is compared with mineral oil. However, the most important difference between esters and mineral oils is in their kinematic viscosity. Because of this, they are not as efficient as mineral oils to remove the heat from the transformer due to a lower oil velocity inside the cooling channels of the windings, around the magnetic core, and inside the radiator fins, reducing the convective heat transfer process. A natural ester, at low temperatures (i.e., $0\,°C$) has a kinematic viscosity $\simeq 900\%$ bigger than mineral oil. This percentage reduces to $\simeq 500\%$ at $20\,°C$ and to $\simeq 50\%$ at $100\,°C$ Santisteban et al. [1]. Consequently, a higher hot spot oil temperature is obtained for the same load and ambient temperature, if compared with mineral oil as a cooling fluid. When the transformer is operated at a very low ambient temperature and is filled with biodegradable oil the pour point of the oil can be reached. The pour point is defined in Data [2] as the lowest temperature at which a fluid is observed to flow under specified conditions (ASTM D97 and ISO 3016 are commonly used test methods). Mineral oils have very low pour point temperatures, below $-40\,°C$, but in the case of conventional sunflower oil can be $-18\,°C$ and the Cargill FR3 $-21\,°C$. As it is mentioned in Data [2] natural ester fluids do not have a well-defined solid/liquid phase transition temperature. When it is operated in very cold temperatures, natural esters gradually increase their viscosity, forming small crystals, but still being able to flow and transfer heat. Another alternative to be used under very cold temperature conditions is the MIDEL 7131, which is a synthetic ester with an extremely low pour point of -56 °C as reported in the thermal properties datasheet Midel_7131 [3]. Therefore, it is necessary to analyze the cooling performance of the esters and the temperature distribution on the active parts of the transformer, when they are used at very low working temperatures.

2 Technical specifications of the distribution transformer

The study is performed on a distribution transformer manufactured by the Tadeo Czerweny S.A. company which has a rated power of $315\,[\mathrm{kVA}]$ with a voltage ratio of $13.2\,[\mathrm{kV}]$ / $0.4\,[\mathrm{kV}]$ and voltage regulation $\pm 2 \times 2.5\%$. A detailed description of the transformer can be found in Garelli et al. [4]. The cooling of the device is realized by natural convection both for the oil inside and for the external air. The transformer is fitted with 16 fins of $605\,[\mathrm{mm}] \times 180\,[\mathrm{mm}]$ size and 48 fins of $605\,[\mathrm{mm}] \times 200\,[\mathrm{mm}]$ size. The interior dimensions of the oil tank are: height $720\,[\mathrm{mm}]$, length $1255\,[\mathrm{mm}]$ and width $410\,[\mathrm{mm}]$. The active part is comprised of three high-voltage (HV) / low-voltage (LV) windings. Pressboard insulation is placed between the HV and LV windings, and also between the LV winding and the magnetic core. Longitudinal channels where the oil flows through the windings are provided in order to increase their cooling. The channels are made by adding $4\,[\mathrm{mm}] \times 4\,[\mathrm{mm}]$ square cross-section pressboard bars or sticks during the manufacturing process (pinpointed as yellow squares in figure 1 (right). These channels are shown in figure 1 (left). The same pressboard bars together with $4\,[\mathrm{mm}]$ thickness pressboard separator sheets are used as an insulator between the HV and LV windings. This is also depicted in figure 1 (right).

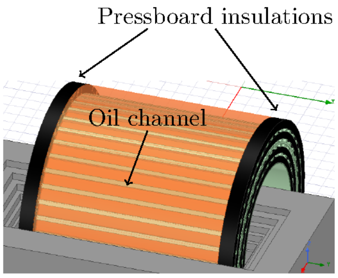

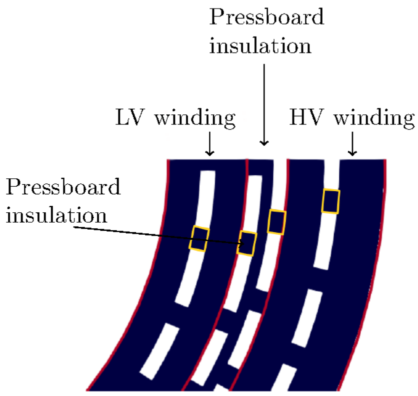

Figure 1. View of the HV and LV windings geometry: detail of the oil channels along the windings (left) and the different insulation materials (right) Garelli et al. [4]

The magnetic core is made of the Fe-Si grain-oriented electrical steel sheets of $0.27\,[\mathrm{mm}]$ thickness. A schematic cross-section on a perpendicular plane to the axis of the windings is shown in figure (2). The cores are wounded as loops or strips (two halves with overlapping ends joined together to form a loop in multiple layers of the wound core). This manner of manufacturing the core is taken into account both in the computation of the magnetic fluxes as well as the thermal conductivity, as will be later explained in the work.

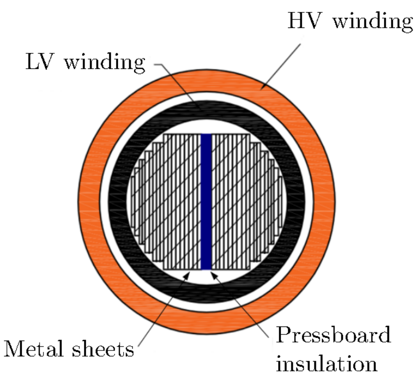

Figure 2. Scheme with cross-section of magnetic core and windings in a normal plane to the windings axis.

It should be mentioned that the pressboard sheets are placed as separators in the gaps between two core loops so that the oil flow is almost blocked in those regions (see detail in the figure 2). Moreover, both the bottom and top ends of the windings are insulated with paper sheets and pressboard ribbons. These insulations are shown in color black in the figure (1)(left).

3 Numerical model

The STEP-format files with the CAD of the geometries for the different parts of the machine were provided by the Tadeo Czerweny S.A. company. The pre-processing of the geometry and the STL mesh generation required by snappyHexMesh OpenFOAM [5] were carried out within the Salome [6] platform. The fluid mesh is generated with snappyHexMesh, which is an open-source, fully parallel, cross-platform library for polyhedra mesh generation implemented within the OpenFOAM®framework.

The domain for the simulations considers only one-quarter of the complete transformer because of the high number of cells that are required to compute accurate results not only of the global variables of interest (e.g. average oil temperature, average heat transfer coefficient, total dissipated power) but also details of the oil flow and temperature distribution at the entrance and inside the channels of the windings, in the small gaps between the core and the LV winding and also inside of each radiator fin. Because one quarter of the complete domain is used, symmetry boundary conditions are applied at the cutting planes. Figure 3 shows a picture of the simulation domain.

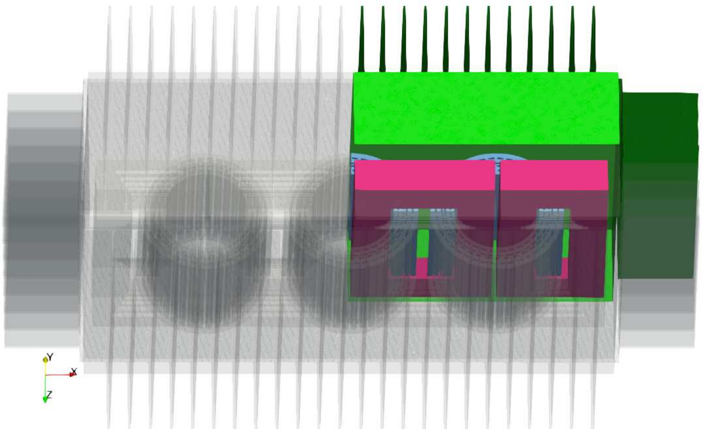

Figure 3. Computational domain (colored) for the thermo-fluid dynamic simulation with Code_Saturn. One-quarter of the full domain is considered.

The meshes for the fluid, windings, and core are made up of polyhedra but they are hexa-dominant, with approximately 35 million cells in total. The number of cells used for the core is approximately 3.1 million and that for the windings is approximately 5.5 million. The meshes are non-conformal at the interfaces between the fluid and the solids. Moreover, special refinement of the fluid mesh is performed near the solid surfaces in order to accurately solve the thermal and fluid boundary layers and thus the heat transfer between the solids and the fluid, particularly at the oil ducts in the windings, where there are approximately 6 or 7 cells in the thickness ($4\,[\mathrm{mm}]$) of the duct. Inside the radiator fins, there are 8 cells in the thickness ($5\,[\mathrm{mm}]$) of the fluid mesh. The refined regions are visible in the figure4. A cut of the core and windings meshes perpendicular to the axis of the windings can be seen in figure **??**. The meshes include those of the pressboard sticks used as separators to generate the oil cooling channels and the pressboard insulation between the LV and HV windings.

The windings (light blue) and the magnetic core (red) are also discretized with FV meshes as shown in Fig. 4, where the heat conduction problem is solved.

The heat losses in the magnetic core and the windings were computed in previous work [4] and these heat losses are used as volume heat source terms. The heat transfer process involves the heat conduction in the core and windings, then the heat dissipates to the oil by conduction and convection, afterward to the walls of the oil tank and the radiator's fins, and finally to the surrounding air. Due to the construction complexity and the use of different materials in the core and windings, an equivalent anisotropic thermal conductivity is used to compute the thermal conduction.

The total power loss provided in the datasheet of the manufacturer is $Q_{Exp} = 4250\,[\mathrm{W}]$ and that computed with the EMAG numerical model described in Garelli et al. [4] is $Q_{EMAG} = 4449\,[\mathrm{W}]$. Because one-quarter of the transformer is considered the total power applied on the model is equal to $Q_{mod} = 1114\,[\mathrm{W}]$.

The heat transfer (convection and radiation) from the walls to the surrounding air is modeled instead of being

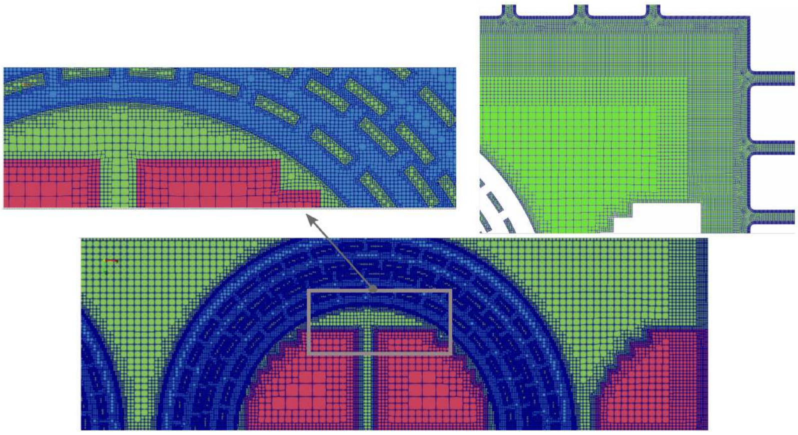

Figure 4. Cut of the fluid and radiator fins meshes. The cutting plane is perpendicular to the axis of the windings (left). Detail of the fluid and the solid meshes at the radiator fins (right).

simulated. This approach is taken since the simulation of the airflow surrounding the transformer would greatly increase the computational cost of the simulations. A detailed description of the modeling process is given in Garelli et al. [4].

Due to the construction complexity of the windings and core, it is not feasible to simulate the heat conduction in the windings and magnetic core with a full representation of the copper wires, paper sheet insulations, small oil gaps between the wires, varnish insulation of the wires or each steel sheets and sheet coating of the magnetic core. Therefore, to take into account the anisotropy in the heat conduction with a reduced computational cost, a procedure is applied in order to compute equivalent thermal conductivities, which are then introduced into the numerical model. A detailed description of the anisotropic thermal conduction properties is given in Garelli et al. [4].

The natural oil flow in the tank simulated by the coupled thermo-hydraulic model is governed by the continuity and momentum conservation equations for unsteady incompressible viscous laminar flows of thermally conducting Newtonian fluids. Under these assumptions, the continuity equation is given by the null divergence of the velocity field

$$\nabla \cdot \boldsymbol{U} = 0 \tag{1}$$

where $\boldsymbol{U} = \boldsymbol{U}(x, y, z, t)$ is the flow velocity field and $\nabla = (\partial/\partial x, \partial/\partial y, \partial/\partial z)$ is the gradient operator. On the other hand, the momentum equation is given by

$$\rho \frac{D\boldsymbol{U}}{Dt} = -\nabla p + \tilde{\rho}(T)\boldsymbol{g} + \nabla \cdot (\mu(T)\nabla \boldsymbol{U}) \tag{2}$$

being $D\boldsymbol{U}/Dt$ is the material or Lagrangian derivative of the velocity field (namely, $D\boldsymbol{U}/Dt = \partial \boldsymbol{U}/\partial t + (\boldsymbol{U} \cdot \nabla)\boldsymbol{U}$), ∇p is the pressure gradient, $\boldsymbol{g}$ is the gravity vector, $\mu(T)$ is the temperature-dependent dynamic viscosity, $\tilde{\rho}(T) = \rho + \Delta\rho$ is the temperature-dependent density and ρ is the reference density value. The temperature-dependence of the density is taken into account only in the source term of the momentum equation using the Boussinesq approximation because the changes in the density are very small ($\Delta\rho/\rho << 0.1$) for the range of operating temperatures of the transformer EDF R&D [7]. However, variation in physical properties like the dynamic viscosity, thermal conductivity, and specific heat are important Le Quéré et al. [8] within this range, so appropriate functions will be later introduced for the physical properties as a function of the temperature for mineral and ester oils.

Additionally, the heat conduction in the solids (windings, core, radiators metal sheets) as well as in the fluid is governed by the Fourier law, namely

$$\boldsymbol{q} = -k(T)\nabla T \tag{3}$$

with k is the thermal conductivity of the media, ∇T is the temperature gradient and $\boldsymbol{q}$ is the heat flow or heat flux density. Finally, the energy conservation equation for incompressible fluids can be stated as follows

$$\rho C_p(T) \frac{DT}{Dt} = \nabla \cdot (k(T)\nabla T) \tag{4}$$

with $C_p(T)$ is the specific heat at constant pressure. The temperature-dependence of the density, viscosity, thermal conductivity, and specific heat will be interpolated for the synthetic ester oil MIDEL 7131 from the datasheet table. These physical properties are shown in the figure 5.

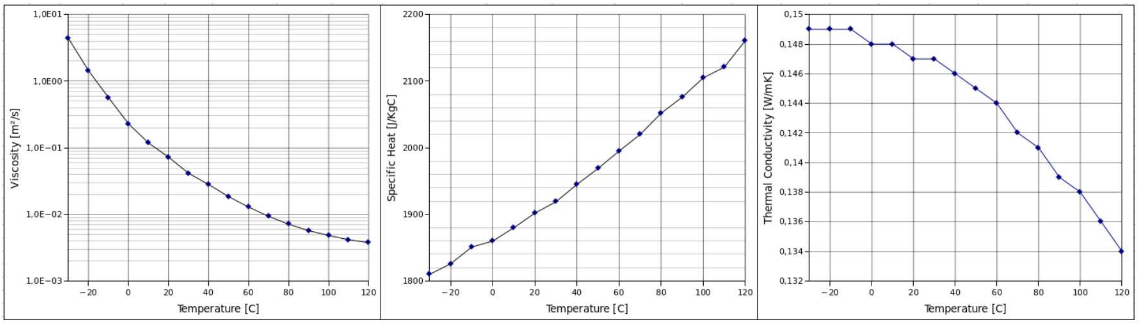

Figure 5. Physical properties MIDEL 7131.

The coupled oil flow and heat transfer problem is numerically solved with the multiphysics parallel scientific code *Code_Saturne* EDF R&D [9], Archambeau et al. [10]. The numerical scheme for space discretization of the unsteady Navier-Stokes equations for incompressible viscous fluid flows is based on the Finite Volume Method (FVM) using the Second Order Linear Upwind (SOLU) Norris [11]. The coupling of the pressure and velocity fields is done with the SIMPLEC algorithm and second order, Crank-Nicholson time integration scheme is used for the transient simulations EDF R&D [7]. The buoyancy of the oil due to the temperature changes is taken into account in the modelization by considering the temperature dependence of the density $\rho_{(T)}$.

4 Results discussion

In this section, the numerical results computed with the coupled TFD simulations with *Code_Saturne* for an ambient temperature of $T_{ext} = -30\,°\mathrm{C}$, is presented. Additionally, the numerical results are compared with the work of Garelli et al. [4], in which an ambient temperature of $T_{ext} = \{30\,°\mathrm{C}\}$ is used.

In figure 6 the location of a cross-section plane in the transformer with the oil temperature distribution and LIC (Line Integral Convolution) vector field to visualize the flow pattern is shown.

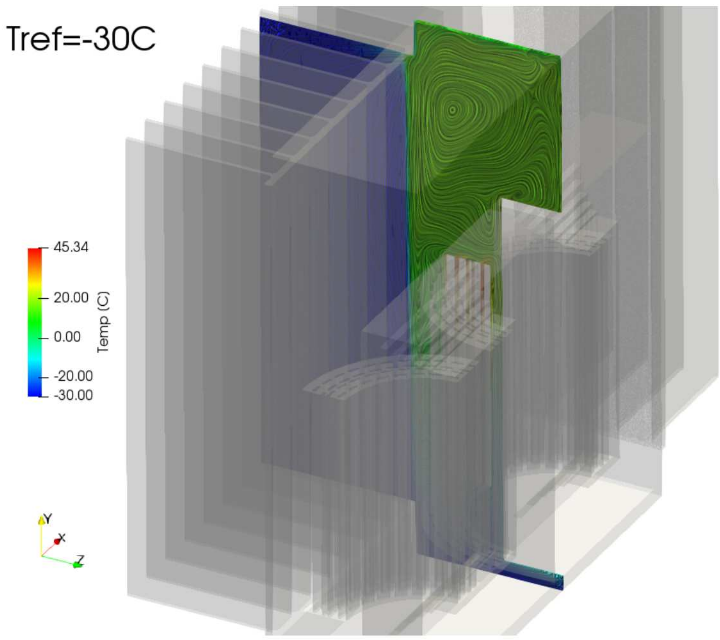

Figure 6. Oil temperature distribution for $T_{ext} = -30\,°\mathrm{C}$.

In figure 7 the results are compared with that obtained for a working temperature of $T_{ext} = 30\,°\mathrm{C}$ in the same plane location that in fig. 6. When the transformer operates at a very low temperature, the higher viscosity reduces the fluid flow through the fins and the oil circulation is concentrated in the upper part. The highest temperatures are located in the winding channels as shown in fig. 8.

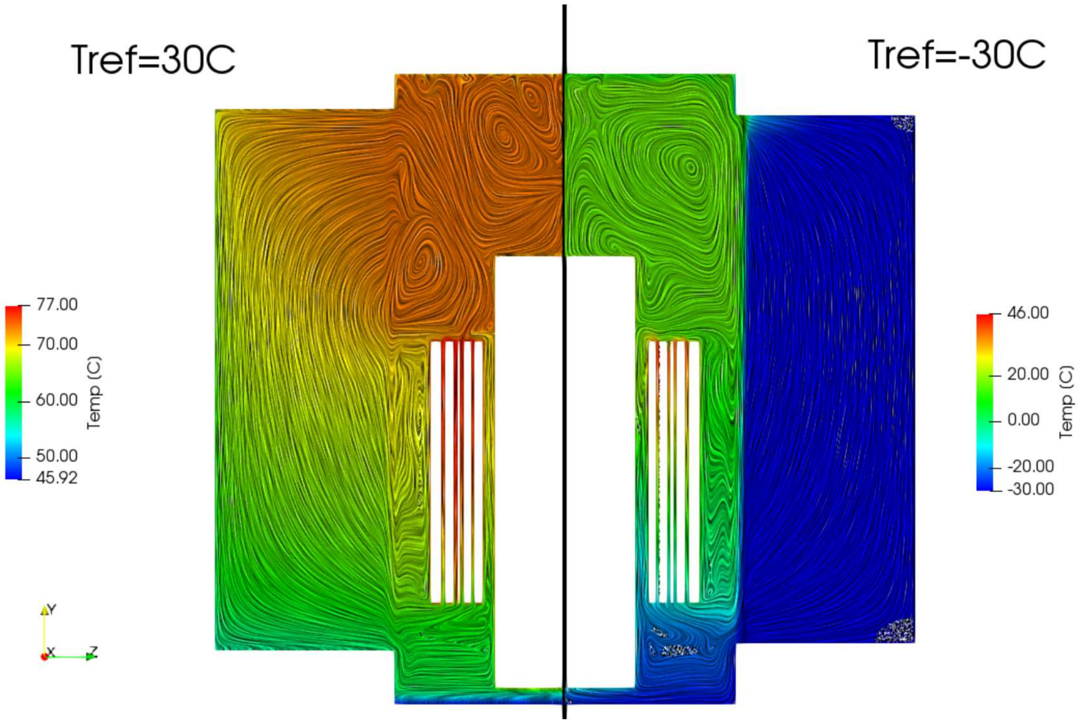

Figure 7. Oil temperature distribution comparison.

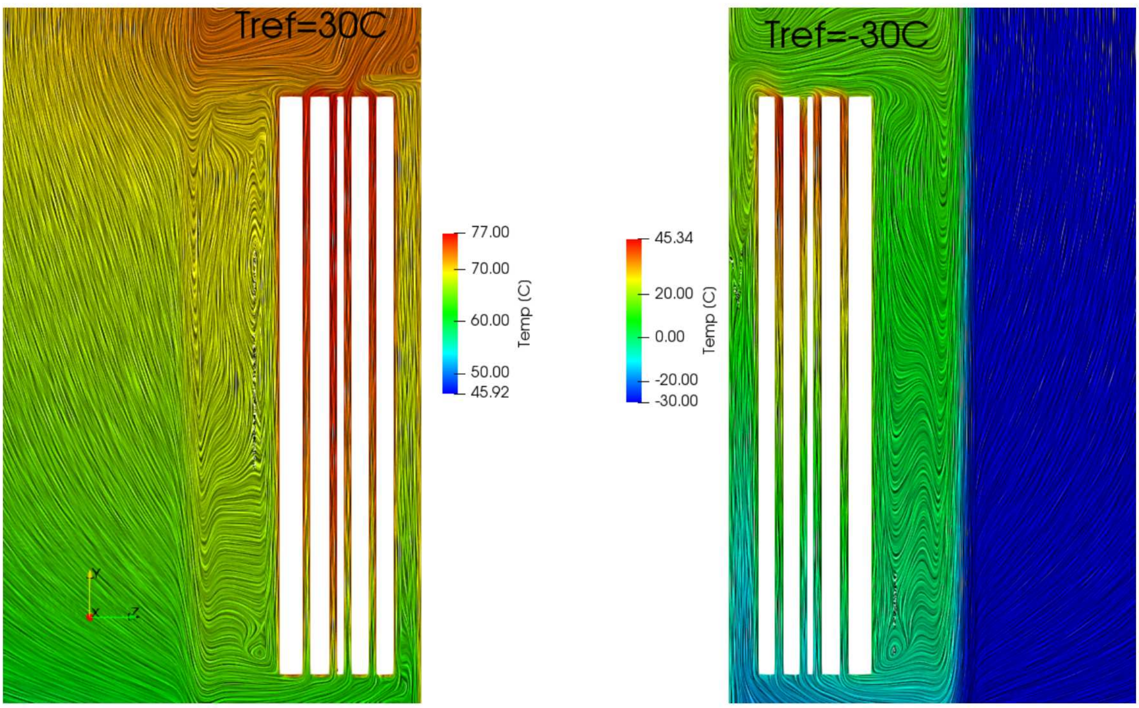

Figure 8. Winding oil channel temperature.

The increase in the kinematic viscosity reduces the oil velocity inside the transformer, reducing the convective heat transfer.

The oil cooling process is mainly produced in the upper part of the transformer, with a very low oil circulation through the fins, as can be noted in fig. 9, where the oil circulation velocity is a few millimeters per second in the fins. Also, the oil velocity is significantly reduced inside of the winding oil channels.

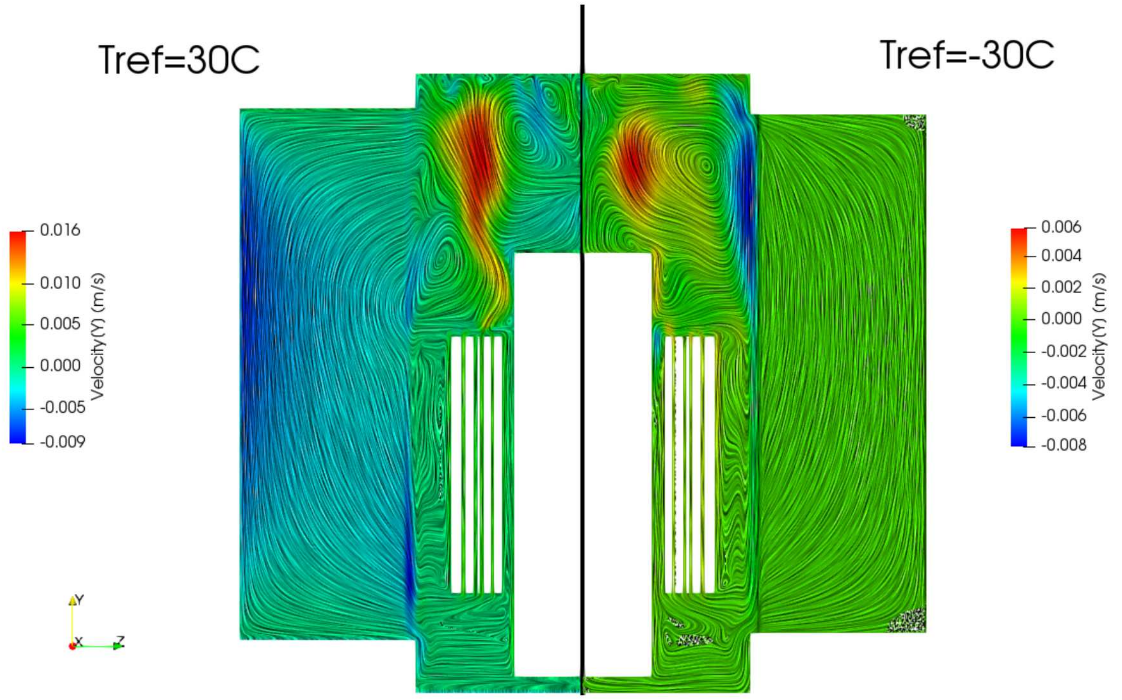

Figure 9. Vertical oil velocity.

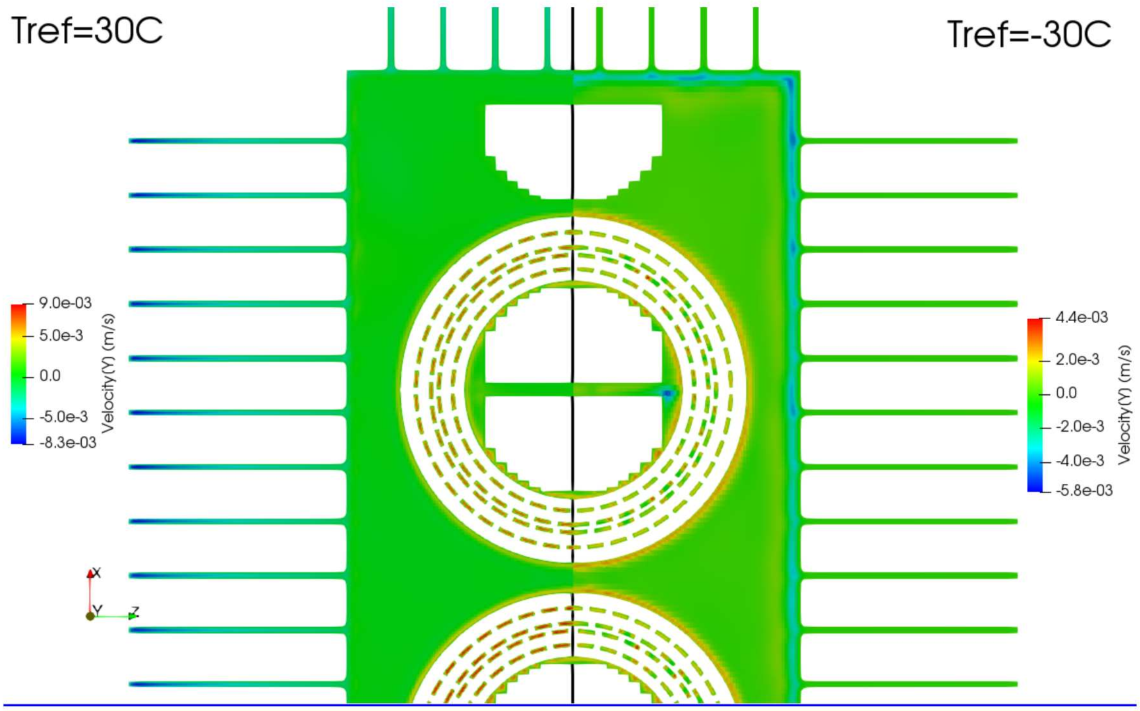

Figure 10. Vertical oil velocity in a horizontal cross-section.

5 Conclusions

In this work, a numerical analysis of a distribution transformer filled with ester oil as a cooling fluid was analyzed. The increase in the kinematic viscosity due to the low ambient temperature reduces the oil velocity inside the oil channels and also inside the fins as was expected. A decrease in the ambient temperature from 30 °C to -30 °C ($\Delta T = -60$ °C) produce a reduction in the hot spot temperature around 30 °C. In both cases, the higher temperatures are located at the outlet region of the winding channels, and the oil cooling process is mainly produced in the upper part of the transformer box, with a very low oil circulation through the fins. The maximum ascending oil velocity is reduced in half in the case of a temperature of -30 °C inside of the oil channels, affecting the convective heat transfer capacity of the oil.

Acknowledgements. This work has received funding from European Union's Horizon 2020 research and innovation program under the Marie Sklodowska-Curie grant agreement No 823969 (BIOTRAFO project of Research and Innovation Staff Exchanges RISE, check https://www.biotrafo.unican.es/, @biotrafo); CAI+D 2020-50620190100140LI, CAI+D 2020-50620190100110LI, PICT-2016-0708, PICT-2018-01607, PICT-2018-02920, PID-UTN-8132.

Authorship statement. The authors hereby confirm that they are the sole liable persons responsible for the authorship of this work, and that all material that has been herein included as part of the present paper is either the property (and authorship) of the authors, or has the permission of the owners to be included here.

References

[1] A. Santisteban, F. O. Fernández, I. F. F. Delgado, A. Ortiz, and C. J. Renedo. Thermal analysis of natural esters in a low-voltage disc-type winding of a power transformer. In *2017 IEEE 19th International Conference on Dielectric Liquids (ICDL)*, pp. 1–4, 2017.
[2] C. R. Data. Cargill Inc., Reference Data R2020 - Envirotemp™FR3™Fluid Behavior in Cold Temperature Environments, 2017.
[3] Midel_7131. Midel 7131 synthetic ester transformer fluid. vol. , 2018.
[4] L. Garelli, G. Ríos Rodriguez, K. Kubiczek, P. Lasek, M. Stepien, J. Smolka, M. Storti, F. Pessolani, and M. Amadei. Thermo-magnetic-fluid dynamics analysis of an onan distribution transformer cooled with mineral oil and biodegradable esters. *Thermal Science and Engineering Progress*, vol. 23, pp. 100861, 2021.
[5] OpenFOAM. *snappyHexMesh - OpenFOAM: User Guide v1912*, 2018.
[6] Salome. Salome: The Open Source Integration Platform for Numerical Simulation. https://www.salome-platform.org/, 2018.
[7] EDF R&D. Code_saturne documentation, 2022a.
[8] P. Le Quéré, R. Masson, and P. Perrot. A Chebyshev collocation algorithm for 2D non-Boussinesq convection. *Journal of Computational Physics*, vol. 103, n. 2, pp. 320 – 335, 1992.
[9] EDF R&D. Code_Saturne an open source CFD software. http://code-saturne.org, 2022b.
[10] F. Archambeau, N. Méchitoua, and M. Sakiz. Code Saturne: A finite volume code for the computation of turbulent incompressible flows - Industrial applications. *International Journal on Finite Volumes*, vol. 1, n. 1, pp. http://www.latp.univ–mrs.fr/IJFV/spip.php?article3, 2004.
[11] S. Norris. *A parallel Navier-Stokes solver for natural convection and free surface flow*. Ph.D. Thesis, Department of Mechanical Engineering, Sydney, 2000.